More accurate generalized gradient approximation for solids

Zhigang Wu* and R. E. Cohen
Carnegie Institution of Washington, Washington, DC 20015, USA
(Received 24 February 2006; published 20 June 2006)

We present a nonempirical density functional generalized gradient approximation (GGA) that gives significant improvements for lattice constants, crystal structures, and metal surface energies over the most popular Perdew-Burke-Ernzerhof (PBE) GGA. The functional is based on a diffuse radial cutoff for the exchange hole in real space, and the analytic gradient expansion of the exchange energy for small gradients. There are no adjustable parameters, the constraining conditions of PBE are maintained, and the functional is easily implemented in existing codes.

DOI: 10.1103/PhysRevB.73.235116 PACS number(s): 71.15.Mb, 71.45.Gm, 77.80.−e

I. INTRODUCTION

Kohn-Sham density functional theory[1,2] (DFT) makes it possible to solve many-electron ground-state problems efficiently and accurately. The DFT is exact if the exchange-correlation (XC) energy E_{XC} were known exactly, but there are no tractable exact expressions of E_{XC} in terms of electron density. Numerous attempts have been made to approximate E_{XC}, starting with the local (spin) density (LSD) approximation (LDA), which is still widely used. The generalized gradient approximations[3–5] (GGAs) are semilocal, seeking to improve upon LSD. Other more complicated approximations are often orbital dependent or/and nonlocal. They suffer from computational inefficiency; it is much harder to treat them self-consistently and to calculate energy derivative quantities.

The XC energy of LSD and GGAs are

$$E_{XC}^{LSD}[n_\uparrow,n_\downarrow]=\int n\epsilon_{XC}^{unif}(n_\uparrow,n_\downarrow)d^3r, \tag{1}$$

and

$$E_{XC}^{GGA}[n_\uparrow,n_\downarrow]=\int f(n_\uparrow,n_\downarrow,\nabla n_\uparrow,\nabla n_\downarrow)d^3r, \tag{2}$$

respectively. Here the electron density $n=n_\uparrow+n_\downarrow$, and ϵ_{XC}^{unif} is the XC energy density for the uniform electron gas. LSD is the simplest approximation, constructed from uniform electron gas, and very successful for solids, where the valence electron densities vary relatively more slowly than in molecules and atoms, for which GGAs (Refs. 5 and 6) achieved a great improvement over LSD. It is well known that LSD underestimates the equilibrium lattice constant a_0 by 1%–3%, and some properties such as ferroelectricity are extremely sensitive to volume. When calculated at the LSD volume, the ferroelectric instability is severely underestimated.[7–9] On the other hand, GGAs tend to expand lattice constants. They well predict correct a_0 for simple metals, such as Na and K,[6] however, for other materials they often overcorrect LSD by predicting a_0 1%–2% bigger[10] than the experiment. Predicting lattice constants more accurately than LSD remains a tough issue, even for state-of-the-art meta-GGAs; nonempirical TPSS (Ref. 11) only achieves moderate improvement over Perdew-Burke-Ernzerhof (PBE), while empirical PKZB (Ref. 12) is worse than PBE. GGAs are especially poor for ferroelectrics, e.g., PBE (Ref. 5) predicts the volume and strain of relaxed tetragonal $PbTiO_3$ more than 10% and 200% too large, respectively,[13] and other GGAs (Refs. 4, 14, and 15) are even worse, as seen in Table I. Another more complicated functional, the nonlocal weighted density approximation (WDA), is also unsatisfactory for this case.[13] To compute these properties correctly, people often constrain volumes at their experimental values V_{expt}. However, V_{expt} is not available for predicting new materials, certain properties are still wrong even at V_{expt}; theoretically it is more satisfactory to do calculations without any experimental data adjustments.

In order to study finite temperature properties, e.g., ferroelectric phase transitions, effective Hamiltonian and potential models, which are used in molecular dynamics (MD) or Monte Carlo (MC) simulations, have been developed with parameters fitted to first-principles results. When the model parameters are fitted to LSD data, these simulations greatly underestimate the phase transition temperatures T_c at ambient pressure,[16–18] and overestimate if fitted to the GGA results.[17] A simple but more accurate approximation for XC energy is necessary.

II. METHODOLOGY

Because the magnitude of the exchange energy is much bigger than correlation in most cases, we focus only on the exchange in this paper. The dimensionless reduced gradient $s=|\nabla n|/[2(3\pi^2)^{1/3}n^{4/3}]$. The exchange enhancement factor F_X is defined as

$$E_X^{GGA}=\int n\epsilon_X^{unif}(n)F_X(s)d^3r, \tag{3}$$

where the exchange energy density of the uniform electron gas $\epsilon_X^{unif}(n)=-\frac{3e^2}{4\pi}(3\pi^2n)^{1/3}$. The PBE ensatz of F_X has the general form

$$F_X=1+\kappa-\kappa/(1+x/\kappa), \tag{4}$$

where $\kappa=0.804$ to ensure the Lieb-Oxford bound,[19] and $x=\mu s^2$ with $\mu=0.21951$ to recover the LSD linear response, i.e., as $s\to 0$, the exchange gradient correction cancels that for correlation. In the range of interest for real systems $0\lesssim s\lesssim 3$, the PBE F_X is a simple numerical fit to that of

TABLE I. Calculated equilibrium volume V_0 (Å^3) and strain (%) of tetragonal $PbTiO_3$ for various GGAs comparing with experimental data at low temperature (see Ref. 26).

	PW91	PBE	revPBE	RPBE	Expt.
V_0	70.78	70.54	74.01	75.47	63.09
Strain	24.2	23.9	28.6	30.1	7.1

PW91, which is constructed from the gradient expansion of a *sharp* real space cutoff of the exchange hole,[4,20] plus some exact constraints.[5] Unlike atoms and molecules, solids can have a *diffuse* tail around the exchange-correlation hole, and a diffuse radial cutoff factor $[1+(u/u_x)^2]\exp[-(u/u_x)^2]$, where u is the distance from the hole center and u_x is the fixed radial cutoff, leads to a smaller F_X (Ref. 20) for $s \gtrsim 1$ than that of the sharp radial cutoff (inset of Fig. 1). This explains why the PBE (PW91) functional improves total energies of atoms and atomization energies of molecules greatly over LSD, but often overcorrects LSD for solids. Two revised versions of PBE, namely revPBE (Ref. 14) with empirical $\kappa=1.245$ and RPBE (Ref. 15) with $F_X=1+\kappa-\kappa\exp(-\mu s^2/\kappa)$, further exaggerate F_X (Fig. 1), giving better energies for atoms and molecules, but worse lattice constants of solids (Table I).

The real space cutoff procedure can only give qualitative features of F_X, not the exact behavior because it depends on the detailed approximations of the procedure and fitting to parameters, so other known constraints must be chosen to determine F_X. Usually valence electron densities of solids vary much more slowly than electron densities of atoms and molecules. The choice of μ in PBE violates the known gradient expansion of Svendsen and von Barth[21] for slowly varying density systems

$$F_X = 1 + \frac{10}{81}p + \frac{146}{2025}q^2 - \frac{73}{405}qp + Dp^2 + O(\nabla^6), \quad (5)$$

where $p=s^2$, $q=\nabla^2 n/[4(3\pi^2)^{2/3}n^{5/3}]$ is the second order reduced gradient, and $D=0$ is the best numerical estimate. If μ is set to $\frac{10}{81}$, F_X of Eq. (4) will be lowered. However the behavior of PBE F_X for small s needs to be retained because (i) it is necessary to retain cancellation of gradient correction of exchange and correlation as $s\to 0$; (ii) F_X determined by a diffuse radial cutoff is close to that by sharp radial cutoff for small s (inset of Fig. 1). Thus we propose the following ensatz for x in Eq. (4):

$$x = \frac{10}{81}s^2 + \left(\mu - \frac{10}{81}\right)s^2\exp(-s^2) + \ln(1+cs^4), \quad (6)$$

where the parameter c is set to recover the fourth order parameters in Eq. (5) for small s. Because a good approximation of q for slowly varying densities is $q\approx\frac{2}{3}p$,[11] $c=\frac{146}{2025}(\frac{2}{3})^2-\frac{73}{405}\frac{2}{3}+(\mu-\frac{10}{81})=0.007\,932\,5$. Our functional will be referred to as "WC," and F_X^{WC} still satisfies the four conditions (d)–(g) constraining F_X^{PBE5}. It is nearly identical to F_X^{PBE} for $s\lesssim 0.5$, and smaller for bigger s, as displayed in Fig. 1. Amazingly, the present simple F_X^{WC} matches that of the more byzantine TPSS meta-GGA for slowly varying densities very well, which makes use of the kinetic energy density to enforce Eq. (5) for small p and q. Contrasting with earlier attempts such as revPBE, WC has no adjustable parameters fitted to experimental data, and it is constructed completely from fundamental physical considerations.

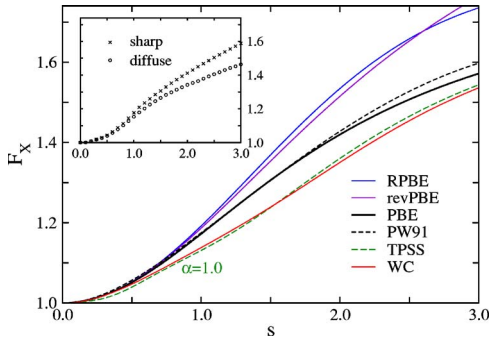

FIG. 1. (Color online) Exchange enhancement factors F_X as functions of the reduced gradient s. The green curve is F_X of TPSS meta-GGA with $\alpha=1.0$, which corresponds to slowly varying density limit. Symbols in the inset are F_X determined by the real-space cutoff procedure. A sharp cutoff generates the crosses, and its parameters are chosen to fit F_X^{PBE}. The circles correspond to a diffuse cutoff with the same parameters.

We tested the functional of Eq. (6) by computing equilibrium crystal structures and cohesive energies of solids, jellium surface energies, and exchange energies of atoms. We used the planewave pseudopotential method (ABINIT4.4.4)[22] for solids, and an all-electron atomic code for atoms. It is straightforward to implement the current GGA from the PBE pseudopotential code. We used the same configurations for each atom to generate optimized norm-conserving pseudopotentials[23] by the OPIUM code[24] of LSD, PBE, and WC.

III. RESULTS AND DISCUSSIONS

A. Solids

First we calculated equilibrium lattice constants a_0 of 18 solids as tested in Refs. 10 and 11. We found LSD underestimates, while PBE overestimates a_0, and current LSD and PBE errors agree well with previous ones. As seen in Table II, WC improves a_0 significantly over LSD and PBE, even much better than TPSS. Note that lattice constants should be extrapolated to 0 K to compare with DFT results due to thermal expansion. An interesting example is a_0 of cubic $PbTiO_3$, which is 3.969 Å at 766 K (ferroelectric phase transition temperature). It reduces to 3.93 Å at 0 K by extrapolation.[26] $a_0^{PBE}=3.971$ Å is 1% larger, whereas $a_0^{WC}=3.933$ Å, in excellent agreement with the extrapolated data. Also note that the zero-point quantum fluctuations are not included in DFT calculations, which would expand a_0 about 0.2%. WC also predicts more accurate bulk moduli for these materials than LSD, PBE, and TPSS (Table III). For cohesive energies,[25] WC is nearly as accurate as PBE, and much better than LSD (Table IV). These results prove that our simple model of GGA is very suitable for solids.

For the ground-state structures of polarized ferroelectrics, the lattice strain must be optimized together with atomic po-

TABLE II. Calculated equilibrium lattice constants a_0 (in Å) of 18 tested solids, comparing with experiments (see Ref. 10). Here the error is the mean absolute relative error, and the TPSS data are from Ref. 10.

	a_0^{LSD}	a_0^{PBE}	a_0^{WC}	a_0^{TPSS}	Expt.
Li	3.401	3.475	3.474	3.475	3.477
Na	4.052	4.198	4.201	4.233	4.225
K	5.045	5.295	5.246	5.362	5.225
Al	3.966	4.062	4.029	4.035	4.032
C	3.536	3.576	3.561	3.583	3.567
Si	5.392	5.475	5.433	5.477	5.430
SiC	4.322	4.387	4.360	4.392	4.358
Ge	5.583	5.782	5.696	5.731	5.652
GaAs	5.584	5.754	5.680	5.702	5.648
NaCl	5.470	5.700	5.622	5.696	5.595
NaF	4.495	4.690	4.632	4.706	4.609
LiCl	4.981	5.164	5.089	5.113	5.106
LiF	3.907	4.061	4.001	4.026	4.010
MgO	4.158	4.249	4.212	4.224	4.207
Cu	3.556	3.668	3.605	3.593	3.603
Rh	3.768	3.849	3.805	3.846	3.798
Pd	3.852	3.963	3.899	3.917	3.881
Ag	4.006	4.164	4.071	4.076	4.069
Error (%)	1.74	1.30	0.29	0.83	

TABLE III. Calculated bulk moduli B_0 (in GPa) of 18 tested solids, comparing with experiments (see Ref. 10). Here the error is the mean absolute relative error, and the TPSS data are from Ref. 10.

	B_0^{LSD}	B_0^{PBE}	B_0^{WC}	B_0^{TPSS}	Expt.
Li	14.6	13.2	12.9	13.2	13.0
Na	9.2	7.8	7.5	7.3	7.5
K	4.4	3.4	3.6	3.6	3.7
Al	83.7	75.9	79.1	84.7	79.4
C	459	428	443	417	443
Si	96.6	87.7	93.3	91.5	99.2
SiC	228	210	219	211	225
Ge	79.0	62.1	68.5	66.2	75.8
GaAs	81.4	64.2	72.8	70.0	75.6
NaCl	32.8	24.2	25.4	22.9	26.6
NaF	62.3	45.8	47.4	43.7	51.4
LiCl	40.7	31.5	34.5	34.1	35.4
LiF	86.4	67.0	70.6	66.5	69.8
MgO	172	149	157	168	165
Cu	178	134	159	171	142
Rh	298	236	271	257	269
Pd	212	152	186	200	195
Ag	131	91.7	110	127	109
Error (%)	12.9	9.9	3.6	7.6	

sitions. Unlike cubic systems, a large volume for a polarized ferroelectric material favors large strain and atomic displacements, and large strain and atomic displacements lead to even larger volumes. This causes PBE to overestimate the volume of tetragonal $PbTiO_3$ by more than 10%, whereas the error is only 3% for the cubic structure. Table V summarizes the LSD, PBE, and WC results of fully relaxed tetragonal $PbTiO_3$ and rhombohedral $BaTiO_3$. It shows that WC predicts highly accurate volumes, strains, and atomic displacements, whereas LSD and PBE underestimate and overestimate these values, respectively. If their model parameters are fitted to first-principles results using WC, MD or MC simulations are expected to determine ferroelectric phase transition temperatures and other properties more accurately.

It is useful to compare the exchange and exchange-correlation potential of LSD, PBE, and WC, as shown in Fig. 2(b) for tetragonal $PbTiO_3$ along the O-Ti bonding ([001]) direction. $V_{\mathrm{X}}^{\mathrm{LSD}}$ is much smoother than $V_{\mathrm{X}}^{\mathrm{GGA}}$, in line with a similar diagram for Si in Ref. 27, which demonstrates that $V_{\mathrm{X}}^{\mathrm{GGA}}$ is much closer to $V_{\mathrm{X}}^{\mathrm{EXX}}$ than $V_{\mathrm{X}}^{\mathrm{LSD}}$ except for the core regions, where GGA exhibits artificial peaks. $V_{\mathrm{X}}^{\mathrm{WC}}$ manages to reduce the PBE peaks around the core regions, and nearly overlaps with $V_{\mathrm{X}}^{\mathrm{PBE}}$ for other regions. Interestingly, Figure 2(c) shows that the difference between $V_{\mathrm{XC}}^{\mathrm{LSD}}$ and $V_{\mathrm{XC}}^{\mathrm{GGA}}$ is much smaller than that between $V_{\mathrm{X}}^{\mathrm{LSD}}$ and $V_{\mathrm{X}}^{\mathrm{GGA}}$ except for the core regions, and this is the lucky cancellation of the LSD exchange and correlation errors making LSD surprisingly accurate for solids. In the core regions with low valence density, $V_{\mathrm{XC}}^{\mathrm{GGA}}$ is significantly less attractive than $V_{\mathrm{XC}}^{\mathrm{LSD}}$,

TABLE IV. Calculated cohesive energies E_{c} (in eV) of 18 tested solids, comparing with experiments (see Ref. 10). Here the error is the mean absolute relative error.

	$E_{\mathrm{c}}^{\mathrm{LSD}}$	$E_{\mathrm{c}}^{\mathrm{PBE}}$	$E_{\mathrm{c}}^{\mathrm{WC}}$	Expt.
Li	1.86	1.61	1.64	1.66
Na	1.22	1.04	1.08	1.13
K	1.02	0.89	0.88	0.94
Al	4.08	3.54	3.84	3.39
C	8.79	7.69	8.09	7.37
Si	5.32	4.61	4.87	4.63
SiC	7.37	6.41	6.73	6.37
Ge	4.78	3.86	4.14	3.87
GaAs	4.23	3.31	3.64	3.35
NaCl	3.59	3.21	3.22	3.31
NaF	4.37	4.05	4.04	3.93
LiCl	3.84	3.44	3.53	3.55
LiF	4.98	4.51	4.58	4.40
MgO	5.68	4.99	5.25	5.22
Cu	4.27	3.27	3.74	3.49
Rh	6.99	5.43	6.25	5.71
Pd	4.68	3.20	3.83	3.89
Ag	3.30	2.39	2.86	2.95
Error (%)	15.2	5.1	5.2	

TABLE V. Equilibrium structural parameters for two ferroelectrics: tetragonal $P4mm$ $PbTiO_3$ (PT) and rhombohedral $R3m$ $BaTiO_3$ (BT). The atom positions u_z are given in terms of the lattice constants.

		LSD	PBE	WC	Expt.
PT	V_0 (Å^3)	60.37	70.54	63.47	63.09[a]
	c/a	1.046	1.239	1.078	1.071[a]
	u_z(Pb)	0.0000	0.0000	0.0000	0.000[b]
	u_z(Ti)	0.5235	0.5532	0.5324	0.538[b]
	$u_z(O_1O_1)$	0.5886	0.6615	0.6106	0.612[b]
	$u_z(O_3)$	0.0823	0.1884	0.1083	0.112[b]
BT	V_0 (Å^3)	61.59	67.47	64.04	64.04[c]
	α	89.91°	89.65°[c]	89.86°	89.87°[c]
	u_z(Ba)	0.0000	0.0000	0.0000	0.000[c]
	u_z(Ti)	0.4901	0.4845	0.4883	0.487[c]
	$u_z(O_1O_1)$	0.5092	0.5172	0.5116	0.511[c]
	$u_z(O_3)$	0.0150	0.0295	0.0184	0.018[c]

[a]Low temperature data, see Ref. 26.
[b]Room temperature data, see Ref. 28.
[c]Low temperature data, see Ref. 29.

causing GGA to expand LSD lattice constants. But the V_{XC}^{PBE} peaks are so high that PBE overcorrects LSD. WC is better than PBE for solids because it lowers these peaks.

It is well known that LSD fails to predict the correct ground states for certain materials, e.g., magnetic bcc iron[30] and α-quartz,[31] and PBE can eliminate this error. WC predicts correct ground states for both iron and quartz with smaller energy differences than PBE, resulting in lower transition pressures. For iron, the transition (bcc to hcp) pressure of 10 GPa is rather close to experiment, but for quartz (α to stishovite), the WC result of 2.6 GPa is not sufficient to correct LSD. Since the stishovite phase is much more compact and stiffer than the α phase, the phonon contributions to energy could increase the energy difference greatly. However, by performing first-principles linear response lattice dynamics calculations we find that the vibration zero point energy difference is only 0.015 eV/SiO_2, because the α phase has high frequency modes the stishovite phase lacks, in addition to low frequency modes. These results indicate that a better correlation functional for WC is also needed.

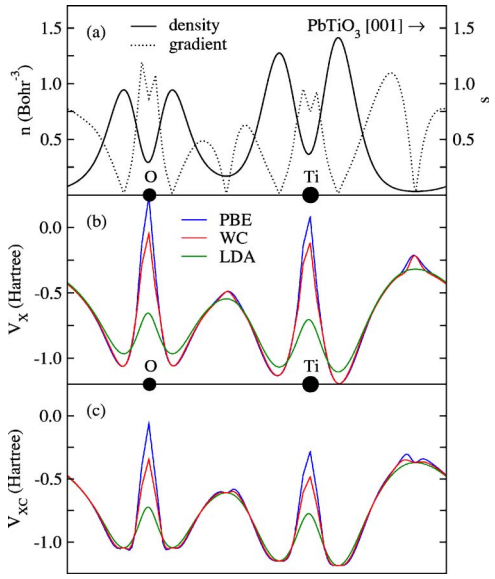

FIG. 2. (Color online) Comparison of LSD, PBE, and WC exchange potential V_X and exchange-correlation potential V_{XC} in tetragonal $PbTiO_3$ along the O-Ti bond axis ([001] direction). All potentials are evaluated with the self-consistent WC density.

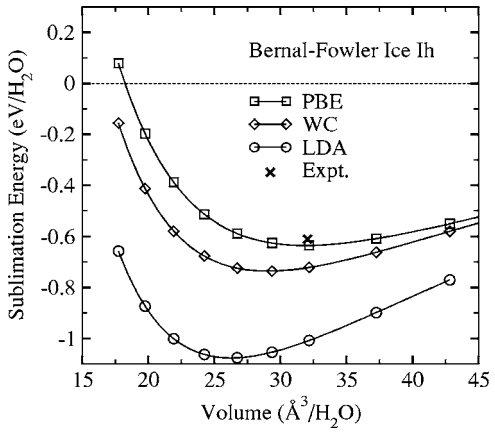

FIG. 3. Sublimation energies of Bernal-Fowler periodic model of ice Ih.

Another interesting case is the weakly interacting molecular bonding systems. We calculated the hydrogen bond strength in ice for a periodic Bernal-Fowler Ih model.[32,33] The WC sublimation energy of 0.73 eV per H_2O (the measured data are 0.61 eV,[34] excluding the zero-point vibration) is much better than LSD of 1.07 eV, but not as good as PBE of 0.63 eV, as shown in Fig. 3.

B. Jellium surface

As argued by Perdew,[2] in an extended system such as metal surface the exact hole may display a diffuse long-tail behavior: an emitted electron's exchange-correlation hole can extend significantly back into the interior of the metal. As summarized in Table VI, jellium surface exchange energy σ_X is severely overestimated by LSD and underestimated by PBE, and σ_X^{WC} are better than both σ_X^{LSD} and σ_X^{PBE}, identical to σ_X^{TPSS} for $r_s \geqslant 3.0$ bohr, where $r_s = (\frac{3}{4\pi n})^{1/3}$. Because the correlation surface energy σ_C^{TPSS} is very close to σ_C^{PBE}, the mean error of σ_{XC}^{WC} against the available most accurate σ_{XC}^{RPA+},[36] which is 1.5%, is comparable to 1.1% of TPSS, better than the LSD and PBE errors of σ_{XC} of 2.1% and 4.9%, respectively. The significant improvement of WC upon PBE for the jellium surface energy is because the diffuse radial cutoff model better describes metal surfaces than the sharp cutoff. The good performance of WC on jellium surface energies suggests it should also perform well on metal vacancies.[37]

C. Atoms

Finally, we compared calculated exchange energies of five noble gas atoms with the Hartree-Fock (HF) results[6] (Table

TABLE VI. Jellium surface exchange energies (σ_X, in erg/cm^2) computed using the LSD orbitals and densities. LSD and PBE values are from Ref. 12, and TPSS values are from Ref. 10. The last row is the mean absolute relative errors against the exact value (see Ref. 35).

r_s (bohr)	LSD	PBE	TPSS	WC	Exact
2.00	3037	2438	2553	2519	2624
2.30	1809	1395	1469	1452	1521
2.66	1051	770	817	809	854
3.00	669	468	497	497	526
3.28	477	318	341	341	364
4.00	222	128	141	141	157
5.00	92	40	47	47	57
6.00	43	12	15	15	22
Error (%)	36.7	16.7	9.4	9.8	

VII). The mean errors for LSD, PBE, RPBE, and WC are 8.77%, 0.89%, 0.18%, and 2.01%, respectively. Comparing the magnitude of F_X of these GGAs as illustrated in Fig. 1, one can conclude that among these choices a GGA with bigger F_X predicts better E_X of atoms. Although WC is constructed for slowly varying densities, it improves exchange energies of atoms over LSD significantly. Furthermore, a proper treatment of the correlation functional would make WC XC energies of atoms as accurate as PBE.

D. Discussions

We have shown that exchange enhancement factors F_X constructed from different situations perform with different accuracy for the same system. Using the PBE correlation functional, WC performs excellently for solids, but it is less accurate for atoms than PBE; on the other hand, RPBE is excellent for atoms, but poorer for solids than PBE. It is difficult to make a GGA which is more accurate than PBE for both solids and atoms simultaneously because F_X is a function *only* of the reduced gradient s. Our calculations show that F_X also depends on the variation of $|\nabla n|$. Since high density systems often have large variations and low density systems often vary slowly, we propose that a GGA having $F_X = F_X(s, r_s)$, just like the gradient correlation correction, could be universally more accurate for atoms, molecules, and solids than PBE. The additional parameters of $F_X(s, r_s)$ can be fitted to quantum Monte Carlo simulations for specific materials, or determined by constraints at $r_s \to 0$ and $r_s \to \infty$ from other theoretical considerations. In addition, a better correlation functional will improve the XC energy and potential also, and one can construct a correlation more compatible with our functional of exchange than PBE. In this way, the accuracy of a simple second rung of the ladder of XC approximations, GGA, could approach that of the more complicated third rung approximation, meta-GGA.

TABLE VII. Exchange energies ($-E_x$, in Ryd) for noble gas atoms calculated from different XC functionals comparing with HF results (see Ref. 6). The last row is the mean abosolute mean errors against HF.

Atom	LSD	PBE	RPBE	New	HF
He	1.723	2.010	2.052	1.962	2.052
Ne	21.933	24.055	24.247	23.737	24.217
Ar	55.623	59.964	60.279	59.372	60.370
Kr	177.071	186.757	187.242	185.716	187.780
Xe	341.026	356.478	357.125	355.016	358.376
Error (%)	8.77	0.89	0.18	2.01	

IV. CONCLUSIONS

We have constructed a GGA which is more accurate for solids than any existing GGA and meta-GGA. It has a very simple form without any empirical parameters, and it is ideal for *ab inito* calculations of certain materials, e.g., ferroelectrics, for which exceptionally high accuracy is needed. It can be generalized to make a GGA more accurate for atoms, molecules, and solids than PBE.

ACKNOWLEDGMENTS

We are indebted to L. Almeida and J. P. Perdew for sending us the jellium code. We thank E. J. Walter, H. Krakauer, P. Schultz, and A. E. Mattsson for helpful discussions. This work was supported by the Center for Piezoelectrics by Design (CPD) and the Office of Naval Research (ONR) under ONR Grant No. N00014-02-1-0506.

*Electronic address: z.wu@gl.ciw.edu; Current address: The Computational Nanoscience Group, University of California at Berkeley, Berkeley, CA 94720, USA.

[1] W. Kohn and L. J. Sham, Phys. Rev. **140**, A1133 (1965).
[2] *A Primer in Density Functional Theory*, edited by C. Fiolhais, F. Nogueira, and M. Marques (Springer, Berlin, 2003).
[3] J. P. Perdew and Y. Wang, Phys. Rev. B **33**, R8800 (1986).
[4] J. P. Perdew, in *Electronic Structure of Solids '91*, edited by P. Ziesche and H. Eschrig (Akademie Verlag, Berlin, 1991).
[5] J. P. Perdew, K. Burke, and M. Ernzerhof, Phys. Rev. Lett. **77**, 3865 (1996).
[6] J. P. Perdew, J. A. Chevary, S. H. Vosko, K. A. Jackson, M. R. Pederson, D. J. Singh, and C. Fiolhais, Phys. Rev. B **46**, 6671 (1992).
[7] R. E. Cohen and H. Krakauer, Phys. Rev. B **42**, 6416 (1990).
[8] R. E. Cohen, Nature (London) **358**, 136 (1992).
[9] D. J. Singh and L. L. Boyer, Ferroelectrics **136**, 95 (1992).
[10] V. N. Staroverov, G. E. Scuseria, J. Tao, and J. P. Perdew, Phys. Rev. B **69**, 075102 (2004).
[11] J. Tao, J. P. Perdew, V. N. Staroverov, and G. E. Scuseria, Phys.

Rev. Lett. **91**, 146401 (2003).
[12] J. P. Perdew, S. Kurth, A. Zupan, and P. Blaha, Phys. Rev. Lett. **82**, 2544 (1999).
[13] Z. Wu, R. E. Cohen, and D. J. Singh, Phys. Rev. B **70**, 104112 (2004).
[14] Y. Zhang and W. Yang, Phys. Rev. Lett. **80**, 890 (1998).
[15] B. Hammer, L. B. Hansen, and J. K. Nørskov, Phys. Rev. B **59**, 7413 (1999).
[16] W. Zhong, D. Vanderbilt, and K. M. Rabe, Phys. Rev. Lett. **73**, 1861 (1994); Phys. Rev. B **52**, 6301 (1995).
[17] M. Sepliarsky, Z. Wu, and R. E. Cohen (unpublished); M. Sepliarsky, Z. Wu, A. Asthagiri, and R. E. Cohen, Ferroelectrics **301**, 55 (2004).
[18] H. Krakauer, R. Yu, C.-Z. Wang, K. M. Rabe, and U. V. Waghmare, J. Phys.: Condens. Matter **11**, 3779 (1999).
[19] E. H. Lieb and S. Oxford, Int. J. Quantum Chem. **19**, 427 (1981).
[20] J. P. Perdew, K. Burke, and Y. Wang, Phys. Rev. B **54**, 16533 (1996).
[21] P. S. Svendsen and U. von Barth, Phys. Rev. B **54**, 17402 (1996).
[22] X. Gonze, J.-M. Beuken, R. Caracas, F. Detraux, M. Fuchs, G.-M. Rignanese, L. Sindic, M. Verstraete, G. Zerah, F. Jollet, M. Torrent, A. Roy, M. Mikami, Ph. Ghosez, J.-Y. Raty, and D. C. Allan, Comput. Mater. Sci. **25**, 478 (2002); http://www.abinit.org
[23] All pseudopotentials were generated with standard radii cutoffs and reference valence configurations, and tested by comparing with previously published LSD and PBE results. Nonlinear core corrections were included in Na and spin-polarized cases. Scalar relativistic potentials were made for atomic numbers bigger than 36. We included semicore states of transition metals as band states. We tested the existence of ghost states and excluded them as local potential. Specifically we used *p* potential as the local potential in the Kleinman-Bylander form for Cu, Rh, Pd, and Ag, *s* potential for Pb.
[24] A. M. Rappe, K. M. Rabe, E. Kaxiras, and J. D. Joannopoulos, Phys. Rev. B **41**, R1227 (1990); http://opium.sourceforge.net.
[25] The ground states of atoms were unconstrained, i. e., spin polarized and nonspherical. The atomic energies were obtained from the DFT-determined ground state configurations, not the experimental ones.
[26] S. A. Mabud and A. M. Glazer, J. Appl. Crystallogr. **12**, 49 (1979).
[27] M. Städele, M. Moukara, J. A. Majewski, P. Vogl, and A. Gorling, Phys. Rev. B **59**, 10031 (1999).
[28] G. Shirane, R. Pepinsky, and B. C. Frazer, Acta Crystallogr. **9**, 131 (1956).
[29] A. H. Hewat, Ferroelectrics **6**, 215 (1974).
[30] L. Stixrude, R. E. Cohen, and D. J. Singh, Phys. Rev. B **50**, 6442 (1994).
[31] D. R. Hamann, Phys. Rev. Lett. **76**, 660 (1996).
[32] D. R. Hamann, Phys. Rev. B **55**, R10157 (1997).
[33] P. J. Feibelman, Science **295**, 99 (2002).
[34] E. Whalley, in *The Hydrogen Bond*, edited by P. Schuster, G. Zundel, and C. Sandorfy (North-Holland, Amsterdam, 1976), Vol. 3, pp. 1425–1470. According to his analysis, zero-point vibration reduces the 0 K sublimation energy of H_2O by 120 meV and of D_2O ice by 98 meV.
[35] J. M. Pitarke and A. G. Eguiluz, Phys. Rev. B **63**, 045116 (2001).
[36] Z. Yan, J. P. Perdew, and S. Kurth, Phys. Rev. B **61**, 16430 (2000).
[37] A. E. Mattsson (private communication).